American Journal of Biological Anthropology

WILEY

AMERICAN JOURNAL OF BIOLOGICAL ANTHROPOLOGY

TECHNICAL NOTE OPEN ACCESS

Compartmentalization Index: Description and Applications in Anthropological Studies

José M. López-Rey[1,2] | Óscar Cambra-Moo[2] | Daniel García-Martínez[2,3,4,5]

[1]Paleoanthropology Group, Department of Paleobiology, National Museum of Natural Sciences (MNCN-CSIC), Madrid, Spain | [2]Laboratorio de Poblaciones del Pasado (LAPP), Department of Biology, Faculty of Sciences, Autonomous University of Madrid (UAM), Madrid, Spain | [3]Physical Anthropology Unit, Faculty of Biological Sciences, Complutense University of Madrid (UCM), Madrid, Spain | [4]Center for Functional Ecology - Science for People and the Planet (CFE). Laboratory of Forensic Anthropology, Centre for Functional Ecology, Department of Life Sciences, University of Coimbra (UC), Coimbra, Portugal | [5]National Center for Research on Human Evolution (CENIEH), Burgos, Spain

Correspondence: José M. López-Rey (jolopezr@mncn.csic.es)

Received: 2 July 2024 | **Revised:** 22 May 2025 | **Accepted:** 17 June 2025

Funding: J.M.L.R. is funded by the Spanish Ministry of Science and Innovation (PRE2021-097584 linked to project PID2020-115854GB-I00). D.G.M. is supported by the Leakey Foundation (Grant 38360 awarded for carrying out the study: "Covariation of internal and external costal anatomy and its importance for understanding the evolution of the human thorax"). The Laboratorio de Poblaciones del Pasado (LAPP) is supported by Projects PGC2018-099405-B-I00 (Spanish Ministry of Science, Innovation and Universities), HAR2016-78036-P (Spanish Ministry of Economy and Competitivity), and SI4/PJI/2024-00104 (Community of Madrid).

Keywords: compartmentalization index | cross section | femur | mineralized area | ontogeny

ABSTRACT

Objectives: The cross-sectional area occupied by mineralized tissues is so high in non-adult individuals that linear methods provide limited information about its variation along their bones. This issue can be addressed using the compartmentalization index, a non-linear index that amplifies differences in cross sections with more than 90% of the mineralized area.

Materials and Methods: We selected five femur diaphyseal cross sections of 35 non-adult *Homo sapiens* individuals from perinatal to 5 years old. Then we measured the percentage of mineralized area of each section and calculated the corresponding compartmentalization index. Subsequently, the distribution of both measurements was graphically tested.

Results and Discussion: As expected, variations of femur diaphyseal mineralized areas are visually magnified using the compartmentalization index for values exceeding 90%, but the significance of statistical comparisons between groups is not affected. This makes the index particularly useful for exploring subtle variations in the early stages of growth and development. In addition, we found that using either the compartmentalization index or direct percentage measurements is equally effective for cross sections with lower mineralized area, as the data distributions are comparable. This also allows applying the compartmentalization index in research focused exclusively on adult individuals.

1 | Introduction

Cross-sectional distribution of mineralized tissues has been largely studied in humans over the last decades. Although it has been mainly assessed on long bones like the femur (Goldman et al. 2009; Sansalone et al. 2012; Wysocki and Doyle 2023) or the humerus (Pfeiffer and Zehr 1996; Cambra-Moo et al. 2014; Pitfield et al. 2017; Zhao et al. 2021), recent publications are using other parts of the skeleton, such as the ribs (García-Martínez et al. 2017; Holcombe et al. 2018; Holcombe et al. 2019; Beresheim et al. 2019; López-Rey et al. 2022, 2023). In general terms, these articles suggest that the distribution of mineralized tissues along adult bones (and their cross sections) is driven by mechanical stress. Therefore,

Summary

- The compartmentalization index is a non-linear method for quantifying cross-sectional mineralized area.
- It amplifies differences in areas with over 90% of mineralized area, typical in non-adults.
- For lower values, it behaves like percentages, making it also applicable to adults.

those regions subjected to higher mechanical forces (e.g., muscular insertions) might have a greater area occupied by mineralized tissues. This is usually measured using linear magnitudes as percentages, which are informative enough when the gradient of mineralized area is variable in the subject of study. However, there are situations where overall bone cross-sectional mineralized area is so high that minimal variations are not evident using linear representations. The most representative case involves the study of bone mineralized area in immature individuals.

It is well-known that there is an inverse relationship between ontogeny and the distribution of bone cross-sectional mineralized area since it is larger in early stages of growth and development. This is due to the abundant woven bone tissue found in infants compared to further ontogenetic stages, when woven bone is replaced by lamellar bone that is mostly concentrated in the peripherical region of the cross sections (Cambra-Moo et al. 2014; García-Martínez et al. 2017; Beresheim et al. 2019). Consequently, mineralized area can reach values over 90% all along the cross sections of the infantile long bones, avoiding the generation of informative graphics on its distribution unless the scale of the "*y* axis" is limited to that percentile. Nevertheless, the percentage of mineralized area (% Min. Ar.) can be easily transformed into a non-linear index that maximizes distribution differences when its value is high enough. This is the case of the compartmentalization index (comp. index, López-Rey et al. 2022, 2023), which is defined as the relationship between the mineralized and non-mineralized areas of the bone cross section according to the following formula, where "*x*" is the % Min. Ar.:

$$\text{Comp. index}\,(y) = \frac{x}{100 - x}$$

Given its mathematical formulation, the comp. index behaves like a rational function whose domain is (0, 99] because (1) cross-sectional mineralized area cannot be 0, (2) cross-sectional mineralized area over 99 would lead to enormous comp. index values, and (3) a cross section 100% mineralized cannot be contemplated since 100/0 is indeterminate. The graphical representation of this rational function results in a hyperbola where '*y*' values increase continuously as '*x*' approaches 99. The obtained hyperbola, however, does not behave as a traditional one because its domain makes it asymmetric, preventing the calculation of a vertex, which could be approximated to '*x*' = 90. The utility of the comp. index is that differences in mineralized area will be exponentially magnified when '*x*' values (% Min. Ar.) are higher than 90, while they will be negligible when '*x*' values are lower (Figure 1). In other words, the comp. index works in the opposite way to a log-transformation: instead of reducing skewness by compressing a wide range of values into a smaller scale (Changyong et al. 2014), it spreads out the otherwise tightly clustered values on the high end of mineralization. This property might help to address the limitations of traditional linear measurements (such as % Min. Ar.) in describing variation within highly mineralized tissues—a challenge that might affect

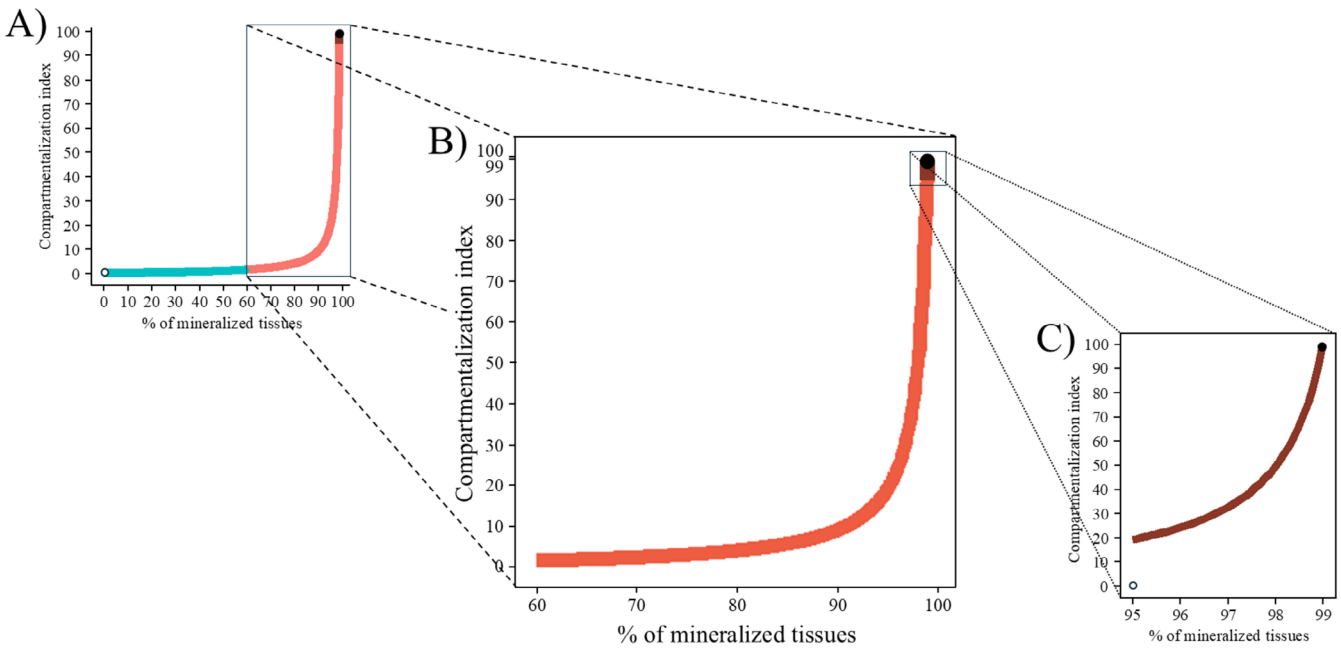

FIGURE 1 | (A) Graphical representation of the compartmentalization index's domain, (B) values of mineralized area contemplated in the selected sample, (C) values where the magnification effects of the compartmentalization index are most pronounced.

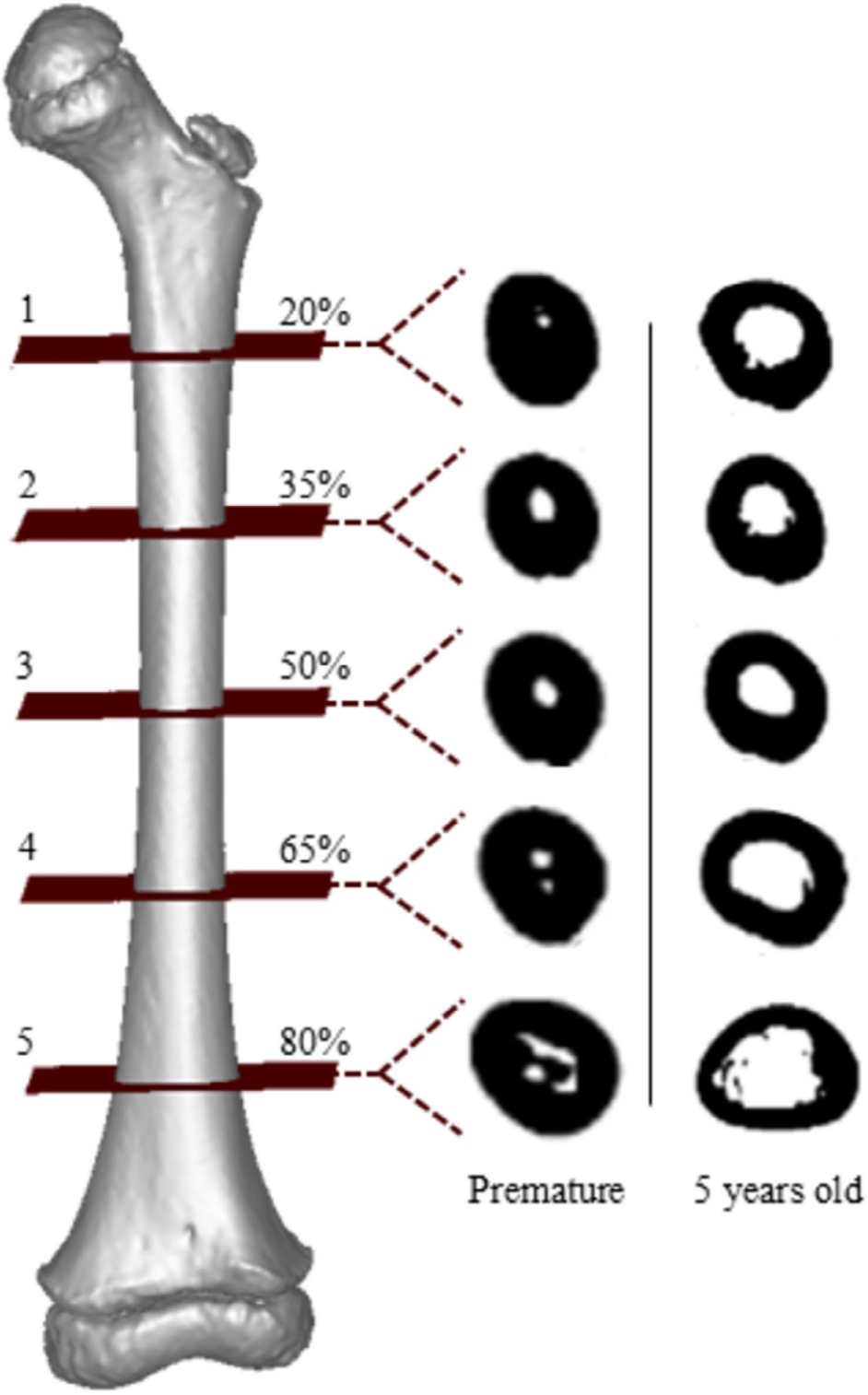

FIGURE 2 | From 1 to 5, numbered cross sections selected along the diaphysis of the left femur belonging to individual ID 110562 (4 years old). The percentage (%) of bone length where each section was obtained is also indicated at the right part of the plane, emulating Gosman et al. (2013). In addition, an example of sections belonging to a random premature and five-year-old individual is included to visually appreciate the magnitude of their differences.

researchers in fields beyond ontogenetic studies, such as comparative anatomy, biomechanics, or paleoanthropology. Thus, this research aims to contrast the classical linear method to the comp. index in order to test whether the latter is more useful for exploring cross-sectional bone properties in early life.

2 | Materials and Methods

The practical case proposed for this methodological article required the CT-scans of 35 non-adult *H. sapiens* masculine individuals, from perinatal to 5 years old, which were requested to the

New Mexico Decedent Image Database (NMDID). Note that perinatal individuals were divided into two groups: "premature" for those who experienced intrauterine fetal death before completing 9 months of pregnancy; and "0" for those who were born after 9 months of pregnancy and passed away before their first year of life. Consequently, the 35 subjects were distributed in seven age-based groups of 5 individuals each. All the sample, whose causes of death did not compromise their skeletal integrity, was scanned using the pediatric OMI protocol (Edgar et al. 2020) with the following parameters: collimation = 16 × 0.75 mm; pitch = 0.938; voltage = 120 kVp; reference tube current-time = 200 mAs; and rotation time = 0.50 s. DICOM images from the CT-scans were transformed into virtual 3D models in Slicer v. 5.6.2 (Fedorov et al. 2012). Afterwards, we segmented the left femur of each individual and selected five equidistant cross sections from the beginning to the end of the femoral diaphysis (Figure 2), such as done by Gosman et al. (2013).

Then we calculated the percentage of each cross section's mineralized area (% Min. Ar.) in Fiji-Image J v. 2.1.0/1.53s (Schindelin et al. 2012). For this purpose, the software provides a threshold for differentiation between bone tissue (mineralized area, including both cortical and trabecular bone) and soft tissue (non-mineralized area). Knowing the total area of each cross section, we determined the % Min Ar. and then used it for computing the corresponding compartmentalization index (comp. index) according to the formula:

$$\text{Comp. index} = \frac{\%\,\text{Min. Ar.}}{100 - \%\,\text{Min. Ar.}}$$

The distribution of the % Min. Ar. and comp. index values (Table 1, SOM Table S1) was depicted by line plots with error bars (Figure 3) and statistically studied by Kruskal–Wallis ($p < 0.05$) + Dunn–Bonferroni *post hoc* tests (Table 2). These analyses were performed in RStudio v. 2023.12.1-402 (R Core Team 2023) using the packages "ggplot2" v. 3.3.3 (Wickham 2016) and "stats" v. 4.2.3 (R Core Team 2023). The full R script is included in Table S1.

3 | Results and Discussion

Figure 3 shows that, on a scale from 0 to 100, the distribution of *Y* values tends to range from 60 to 100 for the percentage of mineralized area (% Min. Ar., Figure 3A1), but from 6 to 0 for the compartmentalization index (comp. index, Figure 3B1). As stated by previous publications (Cambra-Moo et al. 2014; García-Martínez et al. 2017; Beresheim et al. 2019), mineralized area decreases with age, being significantly larger ($p < 0.05$) in most of the cross sections of premature individuals regardless of the method (% Min. Ar., comp. index) used for its quantification (Table 1, Table 2). This is important, as it demonstrates that the comp. index is a useful tool for exploring high % Min. Ar. without inflating *p*-values or altering the statistical significance observed in the raw data. In fact,

TABLE 1 | Mean and standard deviation of each femur cross section's percentage of mineralized area (% Min. Ar.) and compartmentalization index (comp. index) according to age groups.

Age (years)	Section number	% Min. Ar.	Comp. index
Premature (< 9 months of intrauterine development)	1	93.69 ± 5.88	42 ± 42.62
	2	97.08 ± 2.83	58.98 ± 36.86
	3	96.62 ± 3.56	62.89 ± 43.97
	4	94.6 ± 4.59	35.76 ± 33.13
	5	87.27 ± 5.25	8.2 ± 4.15
0 < 12 months (after birth)	1	86.86 ± 1.82	6.75 ± 1.28
	2	91.67 ± 2.21	11.89 ± 4.25
	3	92.81 ± 4.01	15.35 ± 5.58
	4	86.4 ± 7.93	8.32 ± 4.86
	5	80.42 ± 5.91	4.41 ± 1.27
1	1	67.46 ± 8.98	2.28 ± 0.98
	2	84.26 ± 5.84	6.23 ± 3.09
	3	81.92 ± 3.3	4.69 ± 1.07
	4	69.15 ± 2.58	2.26 ± 0.26
	5	62.81 ± 5.28	1.74 ± 0.41
2	1	64.36 ± 7.13	1.88 ± 0.48
	2	79.27 ± 5.45	4.07 ± 1.18
	3	77.14 ± 5.65	3.62 ± 1.26
	4	68.93 ± 8.2	2.44 ± 1.06
	5	62.64 ± 8.52	1.83 ± 0.83
3	1	66.35 ± 5.7	2.06 ± 0.63
	2	79.36 ± 2.44	3.9 ± 0.56
	3	77.67 ± 2.8	3.54 ± 0.61
	4	68.78 ± 5.33	2.28 ± 0.58
	5	60.45 ± 2.31	1.54 ± 0.15
4	1	67.97 ± 11.02	2.38 ± 0.95
	2	78.53 ± 11.49	4.4 ± 1.75
	3	77.5 ± 6.12	3.68 ± 1.08
	4	73.38 ± 4.4	2.84 ± 0.6
	5	68.73 ± 4.79	2.27 ± 0.56
5	1	69.73 ± 5.15	2.38 ± 0.59
	2	77.8 ± 6.27	3.79 ± 1.26
	3	75.66 ± 7.65	3.47 ± 1.45
	4	71.14 ± 5.23	2.57 ± 0.74
	5	63.01 ± 4.79	1.74 ± 0.32

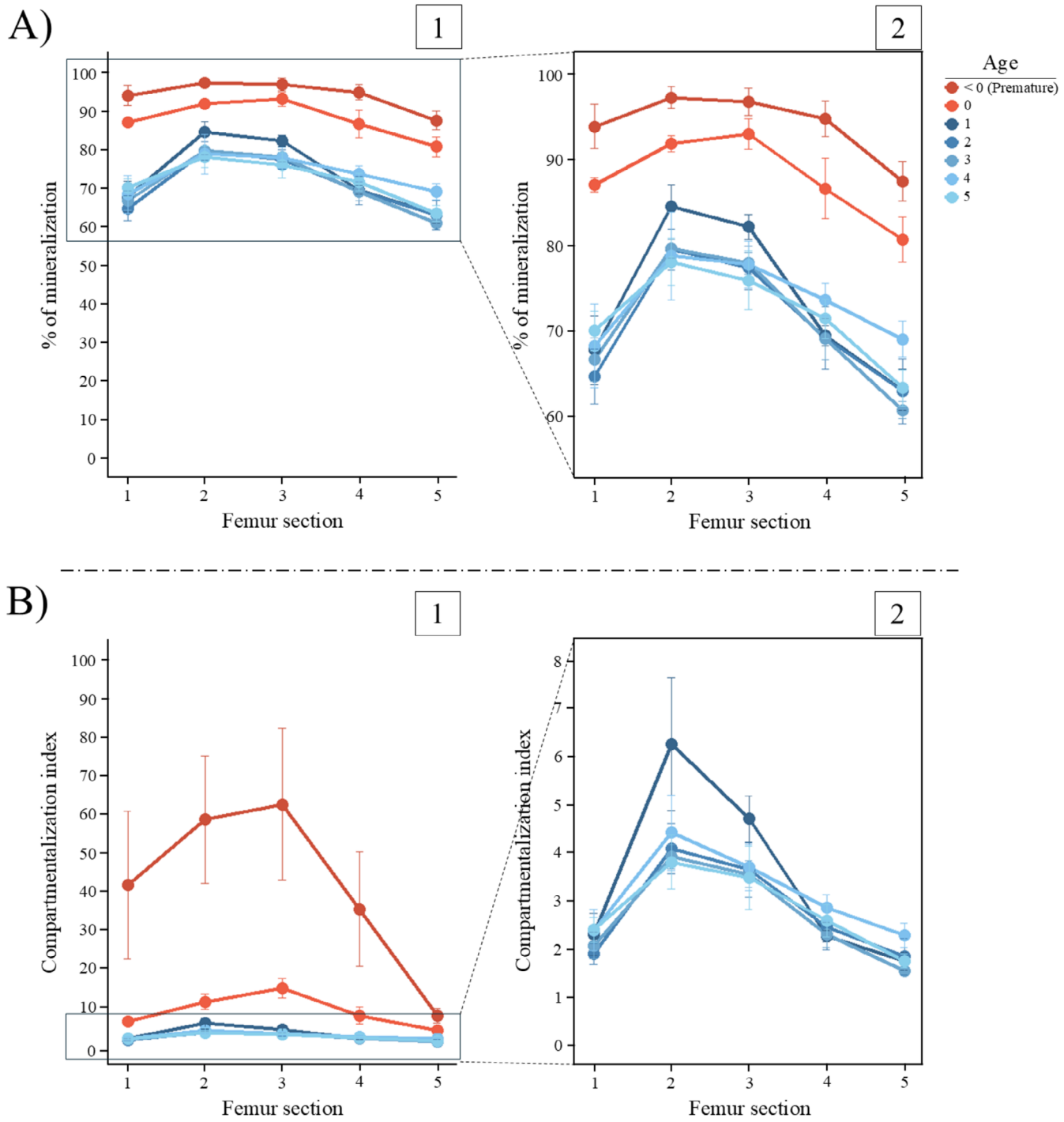

FIGURE 3 | Line plots with standard deviation bars representing the percentage of mineralized tissues (A1) and compartmentalization index (B1) of the studied femur diaphyseal cross sections. A2 and B2 are enlarged sections of the A1 and B1 plots.

the graphical distribution of the values belonging to perinatal individuals is flatter and closer to the rest of the sample in Figure 3A1 than in Figure 3B1, where they are higher and more variable. This is due to the non-linear characteristics of the comp. index (Figure 1), which magnify differences in values over 90% Min. Ar.

Our results also suggest that the relative pattern of change of the % Min. Ar. along the femoral diaphysis is consistent across the whole sample, independent of age, and has two minimum values at the extremes of the diaphysis and one maximum value in its upper half (Table 1, Figure 3). This tendency aligns with previous research on non-adult (Gosman et al. 2013) and adult individuals (Profico et al. 2020). Particularly, on the one hand, minimum % Min. Ar. matches the extremes of the femoral medullar cavity, which are wider than the central part as they contain red bone marrow (hematopoietic) instead of yellow bone marrow (primarily, a reserve) (Guillerman 2013). On the other hand, the maximum % Min. Ar. value might respond to the mechanical stress produced by the insertions of muscles such as the adductors and pectineus on the back of the upper femoral diaphysis (Gray 1918).

TABLE 2 | *p*-value of each Dunn–Bonferroni *post hoc* test.

		Percentage of mineralized area							Compartmentalization index					
		0 y.o.	**1 y.o.**	**2 y.o.**	**3 y.o.**	**4 y.o.**	**5 y o.**		**0 y.o.**	**1 y.o.**	**2 y.o.**	**3 y.o.**	**4 y.o.**	**5 y.o.**
Section 1	1 y.o.	0.18	—	—	—	—	—	1 y.o.	0.18	—	—	—	—	—
	2 y.o.	0.07	1	—	—	—	—	2 y.o.	0.06	1	—	—	—	—
	3 y.o.	**0.03**	1	1	—	—	—	3 y.o.	**0.04**	1	1	—	—	—
	4 y.o.	0.30	1	1	1	—	—	4 y.o.	0.30	1	1	1	—	—
	5 y.o.	0.41	1	1	1	1	—	5 y.o.	0.38	1	1	1	1	—
	Premature	1	**0.047**	**0.015**	**0.006**	0.08	0.12	Premature	1	**0.05**	**0.01**	**0.01**	0.08	0.11
		0 y.o.	**1 y.o.**	**2 y.o.**	**3 y.o.**	**4 y.o.**	**5 y o.**		**0 y.o.**	**1 y.o.**	**2 y.o.**	**3 y.o.**	**4 y.o.**	**5 y.o.**
Section 2	1 y.o.	1	—	—	—	—	—	1 y.o.	1	—	—	—	—	—
	2 y.o.	0.14	1	—	—	—	—	2 y.o.	0.14	1	—	—	—	—
	3 y.o.	0.06	1	1	—	—	—	3 y.o.	0.06	1	1	—	—	—
	4 y.o.	0.56	1	1	1	—	—	4 y.o.	0.56	1	1	1	—	—
	5 y.o.	0.08	1	1	1	1	—	5 y.o.	0.08	1	1	1	1	—
	Premature	1	0.26	**0.014**	**0.005**	0.08	**0.007**	Premature	1	0.26	**0.014**	**0.005**	0.08	**0.007**
		0 y.o.	**1 y.o.**	**2 y.o.**	**3 y.o.**	**4 y.o.**	**5 y o.**		**0 y.o.**	**1 y.o.**	**2 y.o.**	**3 y.o.**	**4 y.o.**	**5 y.o.**
Section 3	1 y.o.	1	—	—	—	—	—	1 y.o.	1	—	—	—	—	—
	2 y.o.	**0.04**	1	—	—	—	—	2 y.o.	0.08	1	—	—	—	—
	3 y.o.	0.10	1	1	—	—	—	3 y.o.	0.09	1	1	—	—	—
	4 y.o.	0.16	1	1	1	—	—	4 y.o.	0.14	1	1	1	—	—
	5 y.o.	0.06	1	1	1	1	—	5 y.o.	**0.05**	1	1	1	1	—
	Premature	1	0.47	**0.008**	**0.02**	**0.04**	**0.012**	Premature	1.000	0.38	**0.017**	**0.019**	**0.03**	**0.011**
		0 y.o.	**1 y.o.**	**2 y.o.**	**3 y.o.**	**4 y.o.**	**5 y o.**		**0 y.o.**	**1 y.o.**	**2 y.o.**	**3 y.o.**	**4 y.o.**	**5 y.o.**
Section 4	1 y.o.	0.14	—	—	—	—	—	1 y.o.	0.15	—	—	—	—	—
	2 y.o.	0.14	1	—	—	—	—	2 y.o.	0.14	1	—	—	—	—
	3 y.o.	0.17	1	1	—	—	—	3 y.o.	0.17	1	1	—	—	—
	4 y.o.	1	1	1	1	—	—	4 y.o.	1	1	1	1	—	—
	5 y.o.	0.15	1	1	1	1	—	5 y.o.	0.47	1	1	1	1	—
	Premature	1	**0.01**	**0.01**	**0.01**	0.31	**0.049**	Premature	1	**0.012**	**0.011**	**0.014**	0.29	**0.05**

(Continues)

TABLE 2 | (Continued)

		0 y.o.	1 y.o.	2 y.o.	3 y.o.	4 y.o.	5 y.o.		0 y.o.	1 y.o.	2 y.o.	3 y.o.	4 y.o.	5 y.o.
Section 5	1 y.o.	0.11	—	—	—	—	—	1 y.o.	0.11	—	—	—	—	—
	2 y.o.	0.06	1	—	—	—	—	2 y.o.	0.06	1	—	—	—	—
	3 y.o.	**0.02**	1	1	—	—	—	3 y.o.	**0.02**	1	1	—	—	—
	4 y.o.	1	1	1	1	—	—	4 y.o.	1	1	1	1	—	—
	5 y.o.	0.17	1	1	1	1	—	5 y.o.	0.17	1	1	1	1	—
	Premature	1	**0.026**	**0.014**	**0.005**	0.72	**0.043**	Premature	1	**0.026**	**0.014**	**0.005**	0.72	**0.043**

Note: Significant *p*-values are highlighted in bold.

Considering this, our experiment demonstrates that the comp. index is a valuable tool for ontogenetic research, particularly for studying individuals in the earliest stages of growth and development. Furthermore, the age range for which the comp. index is useful may depend on the bone selected for the analyses. Since the femoral diaphysis is primarily composed of cortical bone (Goldman et al. 2009; Gosman et al. 2013), % Min. Ar. values decrease rapidly on the ontogenetic scale. Thus, other bones (e.g., vertebrae; Acquaah et al. 2015) or other bone parts (e.g., femur epiphysis; Sansalone et al. 2012) with a higher quantity of trabecular bone in their cross sections might allow for the use of the comp. index for magnifying differences in a more extensive range of ages.

The aforementioned characteristics of the comp. index opens up a wide range of possibilities for using it in research on the human skeleton during ontogeny. For example, future studies could explore whether this method can standardize early bone developmental stages (Cunningham et al. 2016) or detect potential pathologies (Lewis 2017; Welsh and Brickley 2023), which could be helpful in an archaeological context. Given that our results indicate that high levels of cross-sectional % Min. Ar. are observed only in perinatal individuals regarding long bones (Tables 1 and 2, Figure 3), it might be interesting to test whether there is any correlation between mineralization patterns and factors such as intrauterine developmental alterations, maternal diet, or bilateral asymmetries (Namgung and Tsang 2000; Lanham et al. 2008; Nuysink et al. 2008). Traditional linear methods might overlook subtle variations in these cases, whereas exploring these potential associations in both current and archaeological individuals using the comp. index could offer valuable insights into early life conditions and their impact on skeletal development. Furthermore, the utility of the comp. index is not restricted to immature individuals as Figure 3A2, B2 show similar distribution between the % Min. Ar. and the comp. index. Consequently, the latter could be also standardized as a measure of mineralized area in adult bone cross sections (López-Rey et al. 2022, 2023).

4 | Conclusions

The compartmentalization index (comp. index) is a non-linear way to measure the area occupied by mineralized tissues in bone cross sections. It magnifies visual differences when the percentage of mineralized area (% Min. Ar.) is >90%, but does not alter statistical significance of the analyses. This is especially useful in ontogenetic studies at early stages of growth and development, as it might allow for comparisons regarding nutritional or bilateral variables, among others. Furthermore, since data distribution is similar to the % Min. Ar. when values are <80%, the comp. index can also be used as a standard for measuring mineralized area in adult individuals.

Author Contributions

José M. López-Rey: conceptualization (equal), formal analysis (equal), funding acquisition (equal), investigation (equal), methodology (equal), software (equal), visualization (equal), writing – original draft (equal), writing – review and editing (equal). **Óscar Cambra-Moo:** formal analysis (equal), investigation (equal), methodology (equal), supervision

(equal), validation (equal), writing – review and editing (equal). **Daniel García-Martínez:** formal analysis (equal), investigation (equal), methodology (equal), supervision (equal), validation (equal), writing – review and editing (equal).

Acknowledgments

We acknowledge Prof. Armando González Martín for his valuable assistance in refining certain aspects of the manuscript proposal.

Ethics Statement

This research utilizes publicly available data from the New Mexico Decedent Image Database (NMDID). We ensure adherence to ethical standards by respecting data provenance and the rights of individuals included in the sample.

Conflicts of Interest

The authors declare no conflicts of interest.

Data Availability Statement

The data supporting this study's findings come from an open source named New Mexico Decedent Image Database (NMDID). The ID of every individual considered in our research can be obtained from **SOM** Table S1.

References

Acquaah, F., K. A. Robson Brown, F. Ahmed, N. Jeffery, and R. L. Abel. 2015. "Early Trabecular Development in Human Vertebrae: Overproduction, Constructive Regression, and Refinement." *Frontiers in Endocrinology* 6: 136347. https://doi.org/10.3389/fendo.2015.00067.

Beresheim, A. C., S. Pfeiffer, and M. Grynpas. 2019. "Ontogenetic Changes to Bone Microstructure in an Archaeologically Derived Sample of Human Ribs." *Journal of Anatomy* 236, no. 3: 448–462. https://doi.org/10.1111/joa.13116.

Cambra-Moo, O., C. Nacarino Meneses, M. A. Rodríguez Barbero, et al. 2014. "An Approach to the Histomorphological and Histochemical Variations of the Humerus Cortical Bone Through Human Ontogeny." *Journal of Anatomy* 224, no. 6: 634–646. https://doi.org/10.1111/joa.12172.

Changyong, F., W. Hongyue, L. Naiji, et al. 2014. "Log-Transformation and Its Implications for Data Analysis." *Shanghai Archives of Psychiatry* 26, no. 2: 105. https://doi.org/10.3969/j.issn.1002-0829.2014.02.009.

Cunningham, C., L. Scheuer, and S. Black. 2016. *Developmental Juvenile Osteology*. Academic press.

Edgar, H. J. H., S. Daneshvari Berry, E. Moes, N. L. Adolphi, P. Bridges, and K. B. Nolte. 2020. *New Mexico Decedent Image Database*. Office of the Medical Investigator, University of New Mexico. https://doi.org/10.25827/5s8c-n515.

Fedorov, A., R. Beichel, J. Kalpathy-Cramer, et al. 2012. "3D Slicer as an Image Computing Platform for the Quantitative Imaging Network." *Magnetic Resonance Imaging* 30, no. 9: 1323–1341.

García-Martínez, D., O. G. Gil, O. Cambra-Moo, et al. 2017. "External and Internal Ontogenetic Changes in the First Rib." *American Journal of Physical Anthropology* 164, no. 4: 750–762. https://doi.org/10.1002/ajpa.23313.

Goldman, H. M., S. C. McFarlin, D. M. Cooper, C. D. L. Thomas, and J. G. Clement. 2009. "Ontogenetic Patterning of Cortical Bone Microstructure and Geometry at the Human Mid-Shaft Femur." *Anatomical Record* 292, no. 1: 48–64. https://doi.org/10.1002/ar.20778.

Gosman, J. H., Z. R. Hubbell, C. N. Shaw, and T. M. Ryan. 2013. "Development of Cortical Bone Geometry in the Human Femoral and Tibial Diaphysis." *Anatomical Record* 296, no. 5: 774–787. https://doi.org/10.1002/ar.22688.

Gray, H. 1918. *Anatomy of the Human Body*. Lea & Febiger.

Guillerman, R. P. 2013. "Marrow: Red, Yellow and Bad." *Pediatric Radiology* 43: 181–192. https://doi.org/10.1007/s00247-012-2582-0.

Holcombe, S. A., E. Hwang, B. A. Derstine, and S. C. Wang. 2018. "Measuring Rib Cortical Bone Thickness and Cross Section From CT." *Medical Image Analysis* 49: 27–34. https://doi.org/10.1016/j.media.2018.07.003.

Holcombe, S. A., Y. S. Kang, B. A. Derstine, S. C. Wang, and A. M. Agnew. 2019. "Regional Maps of Rib Cortical Bone Thickness and Cross-Sectional Geometry." *Journal of Anatomy* 235, no. 5: 883–891. https://doi.org/10.1111/joa.13045.

Lanham, S. A., C. Roberts, C. Cooper, and R. O. C. Oreffo. 2008. "Intrauterine Programming of Bone. Part 1: Alteration of the Osteogenic Environment." *Osteoporosis International* 19: 147–156. https://doi.org/10.1007/s00198-007-0443-8.

Lewis, M. 2017. *Paleopathology of Children: Identification of Pathological Conditions in the Human Skeletal Remains of Non-Adults*. Academic press.

López-Rey, J. M., Ó. Cambra-Moo, A. González Martín, et al. 2022. "Mineral Content Analysis in the Rib Cross-Sections of *Homo Sapiens* and *pan Troglodytes* and Its Implications for the Study of Sts 14 Costal Remains." *American Journal of Biological Anthropology* 177, no. 4: 784–791.

López-Rey, J. M., Ó. Cambra-Moo, A. González Martín, et al. 2023. "Covariation Between the Shape and Mineralized Tissues of the Rib Cross Section in *Homo Sapiens*, *pan Troglodytes* and Sts 14." *American Journal of Biological Anthropology* 183, no. 1: 157–164. https://doi.org/10.1002/ajpa.24844.

Namgung, R., and R. C. Tsang. 2000. "Factors Affecting Newborn Bone Mineral Content: In Utero Effects on Newborn Bone Mineralization." *Proceedings of the Nutrition Society* 59, no. 1: 55–63. https://doi.org/10.1017/S0029665100000070.

Nuysink, J., I. C. Van Haastert, T. Takken, and P. J. Helders. 2008. "Symptomatic Asymmetry in the First Six Months of Life: Differential Diagnosis." *European Journal of Pediatrics* 167: 613–619. https://doi.org/10.1007/s00431-008-0686-1.

Pfeiffer, S., and M. K. Zehr. 1996. "A Morphological and Histological Study of the Human Humerus From Border Cave." *Journal of Human Evolution* 31, no. 1: 49–59. https://doi.org/10.1006/jhev.1996.0048.

Pitfield, R., J. J. Miszkiewicz, and P. Mahoney. 2017. "Cortical Histomorphometry of the Human Humerus During Ontogeny." *Calcified Tissue International* 101: 148–158. https://doi.org/10.1007/s00223-017-0268-1.

Profico, A., L. Bondioli, P. Raia, P. O'Higgins, and D. Marchi. 2020. "Morphomap: An R Package for Long Bone Landmarking, Cortical Thickness, and Cross-Sectional Geometry Mapping." *American Journal of Physical Anthropology* 174, no. 1: 129–139. https://doi.org/10.1002/ajpa.24140.

R Core Team. 2023. *R: A Language and Environment for Statistical Computing*. R Foundation for Statistical Computing. https://www.R-project.org/.

Sansalone, V., V. Bousson, S. Naili, et al. 2012. "Anatomical Distribution of the Degree of Mineralization of Bone Tissue in Human Femoral Neck: Impact on Biomechanical Properties." *Bone* 50, no. 4: 876–884. https://doi.org/10.1016/j.bone.2011.12.020.

Schindelin, J., I. Arganda-Carreras, E. Frise, et al. 2012. "Fiji: An Open-Source Platform for Biological-Image Analysis." *Nature Methods* 9, no. 7: 676–682. https://doi.org/10.1038/nmeth.2019.

Welsh, H., and M. B. Brickley. 2023. "Pathology Orexpected Morphology? Investigating Patterns of Cortical Porosity and Trabecularization During Infancy and Early Childhood." *The Anatomical Record* 306, no. 2: 354–365. https://doi.org/10.1002/ar.25081.

Wickham, H. 2016. *ggplot2: Elegant Graphics for Data Analysis*. Springer-Verlag.

Wysocki, M. A., and S. T. Doyle. 2023. "Advancing Osteoporosis Evaluation Procedures: Detailed Computational Analysis of Regional Structural Vulnerabilities in Osteoporotic Bone." *Journal of Personalized Medicine* 13, no. 2: 321. https://doi.org/10.3390/jpm13020321.

Zhao, Y., M. Zhou, H. Li, J. He, P. Wei, and S. Xing. 2021. "Biomechanical Evaluation on the Bilateral Asymmetry of Complete Humeral Diaphysis in Chinese Archaeological Populations." *Symmetry* 13, no. 10: 1843. https://doi.org/10.3390/sym13101843.

Supporting Information

Additional supporting information can be found online in the Supporting Information section.